Published paper

Derossi, S., Baca, S.G., Miller, T.A., Adams, H., Jeffery, J.C. and Ward, M.D. (2009) *Formation and structural chemistry of the unusual cyanide-bridged dinuclear species [Ru-2(NN)(2)(CN)(7)](3-)(NN=2,2 '-bipyridine or 1,10-phenanthroline).* Inorganica Chimica Acta, 362 (4). pp. 1282-1288.

http://dx.doi.org/10.1016/j.ica.2008.06.017

Formation and structural chemistry of the unusual cyanide-bridged dinuclear species $[Ru_2(\mathbf{NN})_2(CN)_7]^{3-}$ (**NN** = 2,2'-bipyridine or 1,10-phenanthroline)

Sofia Derossi,[a] Svetlana G. Baca,[a] Thomas A. Miller,[b] Harry Adams,[a]
John C. Jeffery,[b] and Michael D. Ward[a,*]

[a] Department of Chemistry, University of Sheffield, Sheffield S3 7HF (UK). E-mail: m.d.ward@sheffield.ac.uk

[b] School of Chemistry, University of Bristol, Cantock's Close, Bristol BS8 1TS (UK).

Abstract

Crystallisation of simple cyanoruthenate complex anions $[Ru(\mathbf{NN})(CN)_4]^{2-}$ (**NN** = 2,2'-bipyridine or 1,10-phenanthroline) in the presence of Lewis acidic cations such as Ln(III) or guanidinium cations results, in addition to the expected $[Ru(\mathbf{NN})(CN)_4]^{2-}$ salts, in formation of small amounts of salts of the dinuclear species $[Ru_2(\mathbf{NN})_2(CN)_7]^{3-}$. These cyanide-bridged anions have arisen from combination of two monomer units $[Ru(\mathbf{NN})(CN)_4]^{2-}$ following loss of one cyanide, presumably as HCN. The crystal structures of $[Nd(H_2O)_{5.5}][Ru_2(bipy)_2(CN)_7]{\bullet}11H_2O$ and $[Pr(H_2O)_6][Ru_2(phen)_2(CN)_7]{\bullet}9H_2O$ both show that the cyanoruthenate anions form Ru–CN–Ln bridges to the Ln(III) cations, resulting in infinite coordination polymers consisting of fused $Ru_2Ln_2(\mu\text{–}CN)_4$ squares and $Ru_4Ln_2(\mu\text{–}CN)_6$ hexagons which alternate to form a one-dimensional chain. In $[CH_6N_3]_3[Ru_2(bipy)_2(CN)_7]{\bullet}2H_2O$ in contrast the discrete complex anions are involved in an extensive network of hydrogen-bonding involving terminal cyanide ligands, water molecules, and guanidinium cations. In the $[Ru_2(\mathbf{NN})_2(CN)_7]^{3-}$ anions themselves the two **NN** ligands are approximately eclipsed, lying on the same side of the central Ru–CN–Ru axis, such that their peripheries are in close contact. Consequently when **NN** = 4,4'-$^tBu_2$-2,2'-bipyridine the steric bulk of the *tert*-butyl groups prevents formation of the dinuclear anions, and the only product is the simple salt of the monomer, $[CH_6N_3]_2[Ru(^tBu_2bipy)(CN)_4]{\bullet}2H_2O$. We demonstrated by electrospray mass spectrometry that the dinuclear by-product $[Ru_2(phen)_2(CN)_7]^{3-}$ could be formed in significant amounts during synthesis of monomeric $[Ru(phen)(CN)_4]^{2-}$ if the reaction time was too long or the medium too acidic. In the solid state the luminescence properties of $[Ru_2(bipy)_2(CN)_7]^{3-}$ (as its guanidinium salt) are comparable to those of monomeric $[Ru(bipy)(CN)_4]^{2-}$, with a ^{3}MLCT emission at 581 nm.

Introduction

We and others have been interested in the use of $[Ru(bipy)(CN)_4]^{2-}$ and its analogues as components of photoactive supramolecular assemblies [1]. The combination of attractive photophysical properties, sensitivity to its environment, ease of incorporation into multi-component assemblies *via* non-covalent interactions associated with the cyanide groups, all combine to make it an exceptionally useful and versatile complex in this general field [1]. One obvious method by which $[Ru(bipy)(CN)_4]^{2-}$ can be incorporated into polynuclear assemblies is *via* bridging of the cyanide groups to other metal ions, which we have exploited in heterometallic d-f coordination polymers which display Ru(II)→Ln(III) energy-transfer across cyanide bridges [2].

The usual synthesis of $[Ru(bipy)(CN)_4]^{2-}$ involves the prolonged 1:1 reaction of $K_4Ru(CN)_6$ with bipy in aqueous (or aqueous methanol) solution at reflux, at a pH of about 3 [3]. Control of pH is important, as a pH that is too low results in polymeric impurities [3] which require separating from pure $[Ru(bipy)(CN)_4]^{2-}$ chromatographically [4]. In this paper we describe the preparation and some structural and photophysical properties of the smallest of these polymeric impurities, the dinuclear species $[(NC)_3(bipy)Ru(\mu\text{–}CN)Ru(bipy)(CN)_3]^{3-}$ (more conveniently represented as $[Ru_2(bipy)_2(CN)_7]^{3-}$) in which loss of a cyanide group from one $[Ru(bipy)(CN)_4]^{2-}$ unit – presumably as HCN – results in the gap being filled by an N-donor cyanide ligand from another $[Ru(bipy)(CN)_4]^{2-}$ unit. In addition to being of structural interest because of the externally-directed array of six cyanide units, which are available for coordination to either other metal cations or hydrogen-bond donors, the photophysical properties of this new chromophore are also of interest.

A preliminary communication describing one of these structures was published recently [5].

Results and Discussion

We have found that crystalline salts of $[Ru_2(\mathbf{NN})_2(CN)_7]^{3-}$ [**NN** = 2,2'-bipyridine (bipy) or 1,10-phenanthroline (phen)] arise in low yields from slow crystallisation of aqueous solutions of $K_2[Ru(\mathbf{NN})(CN)_4]$ with either Ln(III) cations or the guanidinium cation. These can occur even when the $K_2[Ru(\mathbf{NN})(CN)_4]$ has been thoroughly purified by ion-exchange chromatography and does not contain any $[Ru_2(\mathbf{NN})_2(CN)_7]^{3-}$ at the start of the crystallisation process. Presumably, the formation of crystals containing dinuclear $[Ru_2(\mathbf{NN})_2(CN)_7]^{3-}$ arises from slow loss of HCN from one molecule of a $[Ru(\mathbf{NN})(CN)_4]^{2-}$ unit, followed by coordination of a cyanide N atom from another monomer unit to the resulting vacant coordination site. It is significant that formation of crystals of $[Ru_2(\mathbf{NN})_2(CN)_7]^{3-}$ occurs only when there are Lewis acids present (Ln^{3+} cations, or the guanidinium cation) which will generate H_3O^+ ions in aqueous solution, thereby facilitating loss of a cyanide ligand as HCN.

Crystal structure of $[Nd(H_2O)_{5.5}][Ru_2(bipy)_2(CN)_7]\bullet 11H_2O$

Crystals of $[Nd(H_2O)_{5.5}][Ru_2(bipy)_2(CN)_7]\bullet 11H_2O$ formed in low yield when separate aqueous solutions of $K_2[Ru(bipy)(CN)_4]$ and $Nd(NO_3)_3\bullet 6H_2O$ are allowed to mix slowly. If the mixture is allowed to evaporate too much then crystals of $[\{Ru(bipy)(CN)_4\}_3\{Nd(H_2O)_4\}_2]\bullet 11H_2O$, from direct combination of the $[Ru(bipy)(CN)_4]^{2-}$ anions and Nd^{3+} cations, form in good yield as reported earlier [2a].

$[Nd(H_2O)_{5.5}][Ru_2(bipy)_2(CN)_7]\bullet 11H_2O$ is a complex one-dimensional infinite chain (Figs. 1 – 3), similar to the structure of the Sm(III) analogue that we reported earlier [5]. The $[Ru_2(bipy)_2(CN)_7]^{3-}$ unit has an 'eclipsed' conformation with the two bipy ligands on the same side of the central Ru–CN–Ru axis. Since there will be free rotation of the Ru(II) units about the central cyanide ligand this conformation is unexpected on steric grounds, although there are two factors which might make it favourable. The first is that the resulting overlap of the two bipy ligands may result in some stabilisation due to aromatic π-stacking, although this is likely to be weak given that the Ru(1)•••Ru(2) separation is 5.24 Å, resulting in comparable separation between the bipy ligands (which are not coplanar but inclined towards one another at an angle of 26°). The second factor which may stabilise this eclipsed conformation is an electrostatic one. In the eclipsed arrangement the $[Ru_2(bpy)_2(CN)_7]^{3-}$ unit has its negative charge concentrated to one side, such that it has the maximum possible dipole moment; the alternative conformation, with the bipy units on opposite sides of the central Ru–CN–Ru axis, would be centrosymmetric and have a dipole moment of zero. The high-dipole arrangement will maximise electrostatic interactions with the highly electropositive Ln^{3+} cations in the lattice. We note that assigment of atoms C(4) and N(4) is unclear as theur thermal parameters are similar and inverting the assignment makes no significant difference to the refinement; it is likely that they are disordered.

Each $[Ru_2(bipy)_2(CN)_7]^{3-}$ unit interacts with three (crystallographically equivalent) Nd(1) centres, *via* atoms N(3), N(5) and N(7). The corollary of this is that each Nd(III) centre is coordinated by three cyanide N atoms, from different (but crystallographically equivalent)

$[Ru_2(bpy)_2(CN)_7]^{3-}$ units. The remaining coordination sites around each Nd(1) are occupied by water ligands. There are five water ligands with unit site occupancy, which – together with the three cyanides – form a square antiprismatic coordination environment, with O(2)/O(4)/O(5)/N(5) forming one approximate square plane, and O(1)/O(3)/N(3)/N(7) the other. A sixth water ligand, O(6), occupies a ninth coordination site capping the square antriprism, but with a site occupancy of only 0.5. Thus the Nd(1) ions have coordination geometries of square antiprismatic or capped square antiprismatic in a 1:1 ratio.

The metal-cyanide polymeric framework (Fig. 2) consists of fused squares and hexagons in a step-like motif which alternate to form a one-dimensional chain. The vertices of the 'square' are made up of two Ru centres [Ru(2)] and two Nd(1) centres, whilst the 'hexagons' contain four ruthenium atoms [two Ru(1) and two Ru(2)] and two Nd(1) atoms. Allowing also for the bridging cyanide atoms, these rings contain twelve and eighteen atoms respectively. The Ru•••Nd separations across the cyanide bridges are all very similar, between 5.60 and 5.61 Å. There is, not surprisingly, extensive hydrogen bonding between those cyanides not involved in metal-metal bridging, and water molecules from adjacent Nd(III) ions or in the lattice. Each chain is oriented anti-parallel to its neighbours, with alternating orientations throughout the crystal.

Crystal structure of $[Pr(H_2O)_6][Ru_2(phen)_2(CN)_7]\cdot 9H_2O$

A very similar structure to the one described above was found when $[Ru(phen)(CN)_4]^{2-}$ was crystallised from aqueous solution in the presence of Pr(III), to afford crystals of $[Pr(H_2O)_6][Ru_2(phen)_2(CN)_7]\cdot 9H_2O$ (Fig. 4, 5). Again, this is a minor product which is formed in small amounts when the aqueous solution is not allowed to reduce in volume too much, which results in crystallisation of the $[Ru(phen)(CN)_4]^{2-}$/Pr(III) salt.

The crystal structure shows that two $[Ru(phen)(CN)_4]^{2-}$ units have combined *via* a cyanide bridge, entailing loss of one cyanide ligand from one of the two $[Ru(phen)(CN)_4]^{2-}$ units to generate the dinuclear complex anion $[Ru_2(phen)_2(CN)_7]^{3-}$ which interacts with three different (but crystallographically equivalent) Pr(III) centres. As in the bipyridyl analogue, the phenanthroline units lie on the same side of the Ru–CN–Ru axis such that they are eclipsed, but the Ru(1)•••Ru(2) separation of 5.23 Å precludes any effective π-stacking between them. The structure of the one-dimensional chains is the same as in the bipyridyl analogue, with an alternating array of fused $Ru_2Pr_2(\mu\text{–}CN)_4$ squares and $Ru_4Pr_2(\mu\text{–}CN)_6$ irregular hexagons. The Ru•••Pr separations across the cyanide bridges are all very similar and lie in the range 5.62 – 5.64 Å. The Pr(III) ions are nine-coordinate, from six water ligands as well as the three bridging cyanide ligands. The three cyanide ligands of each $[Ru_2(phen)_2(CN)_7]^{3-}$ unit that are not involved in bridging to other metal ions [N(4), N(9), N(10)] are all involved in hydrogen-bonding to lattice water molecules with non-bonded N•••O separations in the 2.8 – 3 Å range.

Crystal structure of $[CH_6N_3]_3[Ru_2(bipy)_2(CN)_7]{\bullet}2H_2O$

In order to see if formation of cyanide-bridged dimers $[Ru_2(\mathbf{NN})_2(CN)_7]^{3-}$ could be promoted without Lewis-acidic metal ions present, we combined $K_2[Ru(bipy)(CN)_4]$ with guanidinium chloride in water and let crystals grow by slow evaporation. The guanidinium cation is of course an excellent hydrogen-bond donor which has been used extensively in hydrogen-bonded networks [6]. It is an excellent potential source of protons to allow $[Ru(bipy)(CN)_4]^{2-}$ to dimerise with loss of HCN, and we obtained a reasonable crop of crystals of what proved to be $[CH_6N_3]_3[Ru_2(bipy)_2(CN)_7]{\bullet}2H_2O$, consisting of discrete $[Ru_2(bipy)_2(CN)_7]^{3-}$ anions which are hydrogen-bonded to a network of water molecules and guanidinium cations (Figs. 6 – 8). The dinuclear anion has the same basic structure that we saw in the previous examples, with the two bipyridyl ligands attached to the same side of the central Ru–CN–Ru axis and almost perfectly eclipsed (Fig. 6), to give the maximum dipole moment. The Ru•••Ru separation is 5.26 Å and the bridge is near linear, with Ru–C–N and C–N–Ru angles of 176° in each case. As before the planes of the two bipy ligands are not parallel but convergent, with an angle of 27° between them.

These $[Ru_2(bipy)_2(CN)_7]^{3-}$ anions are associated into a linear array *via* hydrogen-bonding between guanidinium cations and the terminal (axial) cyanides N(3) and N(11). There is a set of three guanidinium cations which bridge each adjacent pair of $[Ru_2(bipy)_2(CN)_7]^{3-}$ anions in this way, as shown in Figure 7(a); the non-bonded N(guanidinium)•••N(cyanide) distances are all similar. Thus the three N•••HN interactions between cyanide N(11) and guanidinium atoms N(2G), N(6G) and N(9G) have N•••N separations 2.98, 3.01 and 3.05 Å respectively; the corresponding distances for the hydrogen-bonds between cyanide atom N(3) and guanidinium atoms N(1G), N(4G) and N(7G) are, again, 2.98, 3.01 and 3.05 Å respectively (although this is coincidental as the two sets of three interactions are not symmetrically equivalent).

Fig. 7(b) shows an alternative view, emphasising the H-bonding environment around one $[Ru_2(bipy)_2(CN)_7]^{3-}$ anion. In addition to the three guanidinium units associated with each of the terminal cyanides N(3) and N(11), there is a guanidinium unit [N(4G)/N(5G)/N(6G)] which lies within the central space between cyanide ligands N(5) and

N(9) and forms a bidentate chelating H-bonding interaction with both; cyanide N(5) H-bonds to N(4G) and N(5G) (N•••N separations, 3.11 and 3.04 Å respectively), and cyanide N(9) H-bonds to N(5G) and N(6G) (N•••N separations, 3.03 and 3.11 Å respectively). In addition the water molecules containing O(1) and O(2) play an important role in this H-bonding network, acting as H-bond donors to cyanide atoms N(9) and N(5) respectively (N•••O separations, both 2.86 Å) and H-bond acceptors from two guanidinium units, with these N•••O separations all lying between 2.96 and 2.98 Å.

The overall result is a three-dimensional H-bonded network in which chains of alternating $[Ru_2(bipy)_2(CN)_7]^{3-}$ anions [*cf.* Fig. 7(a)], with their bridging guanidinium cations (aligned along the crystallographic *a* axis), are further cross-linked by additional interactions like those shown in Fig. 7(b). Thus, for example, the guanidinium unit containing N(4G)/N(5G)/N(6G) uses N(4G) and N(6G) as H-bond donors bridging the cyanides of adjacent anions (as in Fig. 7), and uses its other remaining four H-bonds donors [one from N(4G); one from N(6G); two from N(5G) to associate with an anion in an adjacent chain. The overall network structure is shown in Figure 8.

Crystal structure of monomeric $[CH_6N_3][Ru(^tBu_2bipy)(CN)_4]$

All three structures described above have the same basic structure for the dinuclear $[Ru_2(\mathbf{NN})_2(CN)_7]^{3-}$ anion, with the two bipyridyl ligands in a *syn* orientation on the same side of the Ru–CN–Ru bond and more or less eclipsed; the fact that they lean 'inwards' towards each other means that, at the periphery, the C^4 atoms of the pyridyl rings are getting quite close together. For example, in $[CH_6N_3]_3[Ru_2(bipy)_2(CN)_7]•2H_2O$ atoms the C(3)•••C(22) and C(8)•••C(17) separations [between the C^4 atom on one pyridyl ring and the C^4 atom on the ring in the adjacent ligand] are 3.75 and 3.74 Å respectively. It follows that the presence of bulky substituents at the C^4 positions of the pyridyl rings should prevent the dinuclear anions from forming due to the steric hindrance that would result.

To test this we crystallised a mixture of guanidinium chloride and $K_2[Ru(^tBu_2bipy)(CN)_4]$. The crystalline product proved to be – in line with our expectation – the monomer, $[CH_6N_3]_2[Ru(^tBu_2bipy)(CN)_4]•2H_2O$, with no evidence for the cyanide-bridged dimer in either the solid state, or in solution (by mass spectrometry). The structure is shown in Fig. 9. There is disorder involving one of the ^tBu substituents on the $^tBu_2bipy$ ligand, one of the guanidinium units, and a lattice water molecule [O(2)/O(3)], all of which show 50:50 disorder over two sites. However the basic structure is clear, and consists of sheets of $[Ru(^tBu_2bipy)(CN)_4]^{2-}$ anions alternating with sheets containing a hydrogen-bonded array of guanidinium cations and water molecules. All of the cyanide N atoms are involved in close contacts with guanidinium units and water molecules that are indicative of CN•••HN or CN••HO hydrogen-bonding interactions respectively, resulting in a three-dimensional crosslinked network, and likewise guanidinium units are involved in H-bonding contacts with lattice water molecules. Detailed analysis of this is inappropriate given the disorder of one of the guanidinium cations and one lattice water molecule. The most important point is that in this case it appears that the steric bulk of the t-butyl group has prevented formation of any cyanide-bridged dinuclear Ru(II) units of the type $[Ru_2(\mathbf{NN})_2(CN)_7]^{3-}$.

Attempts to synthesise $[Ru_2(\mathbf{NN})_2(CN)_7]^{3-}$ *anions deliberately: mass spectrometry studies in solution*

It was reported a while ago that during syntheses of complexes of the general type $[Ru(\mathbf{NN})(CN)_4]^{2-}$ from $[Ru(CN)_6]^{4-}$ and the diimine ligand (**NN**) in the presence of acid, control of pH is necessary because of the solution is too acidic, unidentified polymeric impurities result [4,5]. Clearly complexes of the type $[Ru_2(\mathbf{NN})_2(CN)_7]^{3-}$ constitute the smallest of these. Having observed formation of dinuclear anions of this type quite by chance in several crystallisations of salts of mononuclear $[Ru(\mathbf{NN})(CN)_4]^{2-}$ species, as described above, we were interested to see if we could prepare the dinuclear species deliberately by carrying out the reaction of $[Ru(CN)_6]^{4-}$ and a diimine ligand (phenanthroline) at a lower pH than usual, and for a longer time than usual.

Under the normal synthetic conditions (pH 3, reflux for 24 h) an ES mass spectrum of the reaction mixture showed strong peaks for the expected product species based on $[Ru(phen)(CN)_4]^{2-}$, associated with different numbers of K^+ ions and/or loss of cyanide ligands. Very weak peaks associated with formation of dinuclear $[Ru_2(phen)_2(CN)_7]^{3-}$ could be seen at *m/z* 902 and 967 (see Table 6). When the reaction was performed at lower pH, or for longer times, or both, the peaks associated with formation of dinuclear $[Ru_2(phen)_2(CN)_7]^{3-}$ increased substantially in their relative intensity in the ES mass spectra. In some cases we could even see in these mass spectra evidence for formation of a trinuclear species, *e.g.* a peak at *m/z* 1299 can be assigned to the species $[Ru_3(phen)_3(CN)_{10}]^{4-}$ in which two $[Ru(phen)(CN)_4]^{2-}$ units are linked *via* bridging cyanides to a central $\{Ru(phen)(CN)_2\}$ unit which has lost two cyanide groups. This would therefore be $[\{(CN)_3(phen)Ru(\mu\text{–}CN)\}\{Ru(phen)(CN)_2\}\{(\mu\text{–}NC)Ru(CN)_3\}]^{4-}$, or an isomer with one or both of the bridging cyanides the other way around (*m/z* calcd. 1299.5 for the most intense component of the isotope envelope).

Attempts to separate $K_3[Ru_2(phen)_2(CN)_7]$ from $K_2[Ru(phen)(CN)_4]$ by chromatography, either on size-exclusion Sephadex (G10) eluting with water, or ion-exchange Sephadex on cationic DEAE-Sephadex eluting with aqueous NaI, were only partially successful. The two fractions ran very close together and although it was possible to isolate fractions that were substantially enriched with $K_3[Ru_2(phen)_2(CN)_7]$ the mass spectrum always showed significant amounts of $K_2[Ru(phen)(CN)_4]$ (which may of course arise from fragmentation of the dinuclear species into $[Ru(phen)(CN)_4]^{2-}$ and $[Ru(phen)(CN)_3]^-$ fragments). We could not therefore isolate a pure sample of $K_3[Ru_2(phen)_2(CN)_7]$ in this way, although its formation (together with that of higher oligomers) is easy to see by ES mass spectrometry (Table 6).

Photophysical properties of the dinuclear anion in the solid state

Given the substantial interest in the photophysical properties of $[Ru(\mathbf{NN})(CN)_4]^{2-}$ complexes [1-4], we were interested to examine the luminescence behaviour of the dinuclear analogues. Although we could not isolate the dinuclear species pure in solution, $[CH_6N_3]_3[Ru_2(bipy)_2(CN)_7]\bullet 2H_2O$ could be readily isolated as crystals which afforded a pure sample of $[Ru_2(bipy)_2(CN)_7]^{3-}$ in the solid state. The luminescence spectrum of this solid showed a strong, broad emission band with a maximum at 581 nm, which is very similar to the emission from $K_2[Ru(bipy)(CN)_4]$ as a microcrystalline powder (λ_{em} = 577 nm). The luminescence decay could be fitted quite well to a single-exponential process with a lifetime of 470 ns, although the fit was better if two components were used: τ_1 = 140 ns (10% of total) and τ_2 = 670 ns (90% of total). Multi-exponential luminescence decay on solid-state samples is a common feature of solid-state samples with cyanometallate luminophores due to the presence of inhomogeneities in the material [2], so the presence of two luminescence components is not surprising. The important point, however, is that the luminescence wavelength and lifetime of the dinuclear anion are similar to those observed for monomeric $K_2[Ru(bipy)(CN)_4]$ [1,3].

Conclusion

In the presence of Lewis-acidic cations, complexes of the form $[Ru(\mathbf{NN})(CN)_4]^{2-}$ (**NN** = bipy, phen) can dimerise with loss of HCN to generate small amounts of cyanide-bridged dimers $[Ru_2(\mathbf{NN})_2(CN)_7]^{3-}$. These dinuclear anions can also be formed as a by-product during preparation of monomeric $[Ru(\mathbf{NN})(CN)_4]^{2-}$ if the reaction is prolonged and too much acid is used. Yields of pure crystalline products are low but the materials have interesting structures, forming cyanide-bridged coordination networks when lanthanide(III) cations are used, and a hydrogen-bonded infinite network when guanidinium is used as the cation. Use of 4,4'-^{t}Bu$_2$-bipyridine as the **NN** ligand in contrast did not generate any such cyanide-bridged dinuclear species, probably because the steric bulk of the ^{t}Bu substituents prevents the necessary close approach of the two diimine ligands which we observe in all of the crystal structures of the dinuclear anion. The solid-state luminescence properties of $[CH_6N_3]_3[Ru_2(bipy)_2(CN)_7]$ •$2H_2O$ are not very different from those of monomeric $[Ru(bipy)(CN)_4]^{2-}$ salts.

Experimental section

Materials and reagents.

$K_2[Ru(bipy)(CN)_4]$ [3], $K_2[Ru(phen)(CN)_4]$ [4] and $K_2[Ru(^tBu_2bipy)(CN)_4]$ [7] were prepared according to the published methods. Other metal salts and reagents were purchased from Aldrich and used as received. Electrospray mass spectra were recorded on a Waters-LCT time-of-flight spectrometer. Luminescence spectra were measured as powdered solids on a Perkin-Elmer LS50B fluorimeter using a front surface accessory; the luminescence lifetime was measured with an Edinburgh Instruments 'Mini-τ' instrument using a 405 nm diode laser as the excitation source.

$[Nd(H_2O)_{5.5}][Ru_2(bipy)_2(CN)_7]$•$11H_2O$

Slow mixing in an H-tube of separate aqueous solutions containing $K_2[Ru(bipy)(CN)_4]$ and $Nd(NO_3)_3$•$6H_2O$ respectively resulted in appearance of a small number of crystals of $[Nd(H_2O)_{5.5}][Ru_2(bipy)_2(CN)_7]$•$11H_2O$ at the interface. IR: ν (cm^{-1}) 3185, 2071, 2030, 1617, 1600, 1468, 1443, 1425, 763, 733.

$[Pr(H_2O)_6][Ru_2(phen)_2(CN)_7]$•$9H_2O$

Slow evaporation of an aqueous acetone (1:1) solution containing $K_2[Ru(phen)(CN)_4]$ and $Pr(NO_3)_3$•$6H_2O$ respectively in an equimolar ratio resulted in appearance of a small number of crystals of $[Pr(H_2O)_6][Ru_2(phen)_2(CN)_7]$•$11H_2O$ after two months.

$[CH_6N_3]_3[Ru_2(bipy)_2(CN)_7]$•$2H_2O$.

Slow evaporation of an aqueous solution of $K_2[Ru(bipy)(CN)_4]$ and guanidine nitrate (in the ratio 1:2) afforded yellow crystals of $[CH_6N_3]_3[Ru_2(bipy)_2(CN)_7]\bullet 2H_2O$. The yield of crystalline material was low (≈ 5%). IR: ν (cm^{-1}) 3342, 3187, 2094, 2059, 2034, 1652, 1580, 1444, 1343, 1157, 823, 763, 733.

$[CH_6N_3]_2[Ru(^tBu_2bipy)(CN)_4]\bullet 2H_2O$

Slow evaporation of an aqueous solution of $K_2[Ru(^tBu_2bipy)(CN)_4]$ and guanidine nitrate (in the ratio 1:2) afforded orange crystals of $[CH_6N_3]_3[Ru_2(bipy)_2(CN)_7]\bullet 2H_2O$. Anal. found C, 48.4; H, 6.2; N, 28.2; the dehydrated material $[CH_6N_3]_3[Ru_2(bipy)_2(CN)_7]$ requires C, 48.6; H, 6.1; N, 28.3%. IR: ν (cm^{-1}) 3390, 3116, 2964, 2097, 2060, 2030, 1654, 1612, 1543, 1480, 1410, 1366, 1250, 1201, 899, 854, 841, 750.

X-ray Crystallography.

X-ray crystallographic data are summarised in Table 5. In each case a suitable crystal was coated with hydrocarbon oil and attached to the tip of a glass fibre and transferred to a Bruker APEX-2 CCD diffractometer (graphite monochromated Mo-Kα radiation, λ = 0.71073 Å) under a stream of cold N_2. After collection and integration the data were corrected for Lorentz and polarisation effects and for absorption by semi-empirical methods (SADABS) [8] based on symmetry-equivalent and repeated reflections. The structures were solved by direct methods or heavy atom Patterson methods and refined by full matrix least squares methods on F^2. Hydrogen atoms were placed geometrically and refined with a riding model and with U_{iso} constrained to be 1.2 (1.5 for methyl groups) times U_{eq} of the carrier atom. Structures were solved and refined using the SHELX suite of programs [9]. Significant bond distances and angles for the structures of the metal complexes are in Tables 1 – 4.

Acknowledgements

We thank the European Commission for a Marie-Curie post-doctoral fellowship to S. G. B. (contract M1F1-CT-2005-513860), and the Universities of Sheffield and Bristol, for financial support.

References

[1] M. D. Ward, Coord. Chem. Rev. 250 (2006) 3128.

[2] (a) G. M. Davies, S. J. A. Pope, H. Adams, S. Faulkner, M. D. Ward, Inorg. Chem. 44 (2005) 4656,

(b) H. Adams, W. Z. Alsindi, G. M. Davies, M. B. Duriska, T. L. Easun, H. E. Fenton, J.-M. Herrera, M. W. George, K. L. Ronayne, X.-Z. Sun, M. Towrie, M. D. Ward, Dalton Trans. (2006) 39.

(c) J.-M. Herrera, S. J. A. Pope, H. Adams, S. Faulkner, M. D. Ward, Inorg. Chem. 45 (2006) 3895.

(d) S. G. Baca, H. Adams, D. Sykes, S. Faulkner, M. D. Ward, Dalton Trans. (2007) 2419.

(e) J.-M. Herrera, S. J. A. Pope, A. J. H. M. Meijer, T. L. Easun, H. Adams, W. Z. Alsindi, X.-Z. Sun, M. W. George, S. Faulkner, M. D. Ward, J. Am. Chem. Soc. 129 (2007) 11491.

[3] J. L. Habib Jiwan, B. Wegewijs, M. T. Indelli, F. Scandola, S. E. Braslavsky, Recl. Trav. Chim. Pays-Bas 114 (1995) 542.

[4] M. Kovács, A. Horvath, Inorg. Chim. Acta 335 (2002) 69.

[5] T. A. Miller, J. C. Jeffery, M. D. Ward, CrystEngComm. 5 (2003) 495.

[6] (a) K. T. Holman, A. M. Pivovar, J. A. Swift, M. D. Ward, Acc. Chem. Res. 34 (2001) 107.

(b) V. Videnova-Adrabinska, E. Obara, T. Lis, New J. Chem. 31 (2007) 287.

(c) N. J. Burke, A. D. Burrows, M. F. Mahon, J. E. Warren, CrystEngComm 8 (2006) 931.

(d) F. F. Said, T.-G. Ong, P. Bazinet, G. P. A. Yap, D. S. Richeson, Cryst. Growth Des. 6 (2006) 1848.

[7] S. Derossi, H. Adams, M. D. Ward, Dalton Trans. (2007) 33.

[8] G. M. Sheldrick: SADABS, A program for absorption correction with the Siemens SMART area-detector system; University of Göttingen (1996).

[9] G. M. Sheldrick: SHELXS-97 and SHELXL-97, programs for crystal structure solution and refinement; University of Göttingen (1997).

Captions for Figures

Fig. 1 ORTEP view of the asymmetric unit of $[Nd(H_2O)_{5.5}][Ru_2(bipy)_2(CN)_7]\bullet 11H_2O$; lattice solvent molecules are omitted, and two additional atoms from adjacent asymmetric units are shown to complete the coordination around Nd(1).

Fig. 2 Structure of the cyanide-bridged chain structure in $[Nd(H_2O)_{5.5}][Ru_2(bipy)_2(CN)_7]\bullet 11H_2O$

Fig. 3 An alternative view looking along a chain in the structure of $[Nd(H_2O)_{5.5}][Ru_2(bipy)_2(CN)_7]\bullet 11H_2O$

Fig. 4 ORTEP view of the asymmetric unit of $[Pr(H_2O)_6][Ru_2(phen)_2(CN)_7]\bullet 9H_2O$; lattice solvent molecules are omitted, and two additional atoms from adjacent asymmetric units are shown to complete the coordination around Pr(1).

Fig. 5 Structure of the cyanide-bridged chain structure in $[Pr(H_2O)_6][Ru_2(phen)_2(CN)_7]\bullet 9H_2O$

Fig. 6 ORTEP view of the asymmetric unit of $[CH_6N_3]_3[Ru_2(bipy)_2(CN)_7]\bullet 2H_2O$

Fig. 7 Two viewss showing the hydrogen-bonding network involving guanidinium cations, water molecules and cyanometallate anions in $[CH_6N_3]_3[Ru_2(bipy)_2(CN)_7]\bullet 2H_2O$

Fig. 8 A view of the overall lattice packing in $[CH_6N_3]_3[Ru_2(bipy)_2(CN)_7]\bullet 2H_2O$

Fig. 9 ORTEP view of the asymmetric unit of $[CH_6N_3]_2[Ru({}^tBu_2bipy)(CN)_4]\bullet 2H_2O$

Table 1. Selected bond distances (Å) and angles (˚) for the structure of $[Nd(H_2O)_{5.5}][Ru_2(bipy)_2(CN)_7]\cdot 11H_2O$

Ru(1)-C(3)	1.968(6)	Nd(1)-O(3)	2.446(6)
Ru(1)-C(1)	2.002(6)	Nd(1)-O(1)	2.448(5)
Ru(1)-C(2)	2.002(6)	Nd(1)-O(4)	2.456(5)
Ru(1)-N(4)	2.081(6)	Nd(1)-O(2)	2.484(4)
Ru(1)-N(22)	2.113(5)	Nd(1)-N(3B)	2.486(6)
Ru(1)-N(11)	2.123(5)	Nd(1)-O(5)	2.507(5)
Ru(2)-C(5)	1.978(6)	Nd(1)-N(5A)	2.527(5)
Ru(2)-C(7)	1.977(6)	Nd(1)-O(6)	2.63(2)
Ru(2)-C(6)	2.011(6)	Nd(1)-N(7)	2.509(5)
Ru(2)-N(31)	2.105(5)		
Ru(2)-N(42)	2.127(5)		
Ru(2)-C(4)	2.063(5)		

C(3)-Ru(1)-C(1)	87.1(3)	C(5)-Ru(2)-C(7)	91.0(2)
C(3)-Ru(1)-C(2)	90.2(3)	C(5)-Ru(2)-C(6)	87.6(2)
C(1)-Ru(1)-C(2)	92.1(3)	C(7)-Ru(2)-C(6)	89.5(2)
C(3)-Ru(1)-N(4)	94.6(3)	C(5)-Ru(2)-C(4)	92.5(2)
C(1)-Ru(1)-N(4)	177.4(2)	C(7)-Ru(2)-C(4)	90.7(2)
C(2)-Ru(1)-N(4)	89.8(2)	C(6)-Ru(2)-C(4)	179.8(2)
C(3)-Ru(1)-N(22)	174.4(2)	C(5)-Ru(2)-N(31)	95.5(2)
C(1)-Ru(1)-N(22)	91.5(2)	C(7)-Ru(2)-N(31)	173.2(2)
C(2)-Ru(1)-N(22)	95.3(2)	C(6)-Ru(2)-N(31)	92.6(2)
N(4)-Ru(1)-N(22)	86.7(2)	C(4)-Ru(2)-N(31)	87.27(19)
C(3)-Ru(1)-N(11)	97.5(2)	C(5)-Ru(2)-N(42)	172.8(2)
C(1)-Ru(1)-N(11)	92.5(2)	C(7)-Ru(2)-N(42)	96.2(2)
C(2)-Ru(1)-N(11)	171.2(2)	C(6)-Ru(2)-N(42)	92.4(2)
N(4)-Ru(1)-N(11)	85.35(19)	C(4)-Ru(2)-N(42)	87.5(2)
N(22)-Ru(1)-N(11)	77.15(19)	N(31)-Ru(2)-N(42)	77.25(19)

Symmetry transformations used to generate equivalent atoms. A: -x+1,-y+2,-z+1. B: x+1,y,z

Table 2. Selected bond distances (Å) and angles (°) for the structure of $[Pr(H_2O)_6][Ru_2(phen)_2(CN)_7]•9H_2O$

Ru(1)-C(5)	1.952(10)	Pr(1)-O(4)	2.459(8)
Ru(1)-C(7)	1.972(10)	Pr(1)-N(1B)	2.514(8)
Ru(1)-C(6)	2.001(11)	Pr(1)-N(7)	2.518(8)
Ru(1)-C(4)	2.033(9)	Pr(1)-O(3)	2.520(10)
Ru(1)-N(31)	2.111(7)	Pr(1)-O(6)	2.522(10)
Ru(1)-N(42)	2.135(7)	Pr(1)-O(1)	2.531(12)
Ru(2)-C(3)	1.956(11)	Pr(1)-N(5A)	2.538(9)
Ru(2)-C(1)	1.977(10)	Pr(1)-O(2)	2.542(8)
Ru(2)-C(2)	2.017(11)	Pr(1)-O(5)	2.618(8)
Ru(2)-N(4)	2.089(10)		
Ru(2)-N(22)	2.108(7)		
Ru(2)-N(11)	2.127(8)		

C(5)-Ru(1)-C(7)	89.4(4)	C(3)-Ru(2)-C(1)	88.8(4)
C(5)-Ru(1)-C(6)	87.4(4)	C(3)-Ru(2)-C(2)	90.5(4)
C(7)-Ru(1)-C(6)	89.8(4)	C(1)-Ru(2)-C(2)	87.0(4)
C(5)-Ru(1)-C(4)	92.4(4)	C(3)-Ru(2)-N(4)	89.9(4)
C(7)-Ru(1)-C(4)	91.8(4)	C(1)-Ru(2)-N(4)	94.1(3)
C(6)-Ru(1)-C(4)	178.3(4)	C(2)-Ru(2)-N(4)	178.8(3)
C(5)-Ru(1)-N(31)	95.8(3)	C(3)-Ru(2)-N(22)	95.4(4)
C(7)-Ru(1)-N(31)	174.2(3)	C(1)-Ru(2)-N(22)	175.8(3)
C(6)-Ru(1)-N(31)	92.9(3)	C(2)-Ru(2)-N(22)	93.2(3)
C(4)-Ru(1)-N(31)	85.4(3)	N(4)-Ru(2)-N(22)	85.7(3)
C(5)-Ru(1)-N(42)	173.3(3)	C(3)-Ru(2)-N(11)	173.6(3)
C(7)-Ru(1)-N(42)	97.0(3)	C(1)-Ru(2)-N(11)	97.6(3)
C(6)-Ru(1)-N(42)	90.7(3)	C(2)-Ru(2)-N(11)	90.8(3)
C(4)-Ru(1)-N(42)	89.3(3)	N(4)-Ru(2)-N(11)	88.7(3)
N(31)-Ru(1)-N(42)	77.9(3)	N(22)-Ru(2)-N(11)	78.3(3)

Symmetry transformations used to generate equivalent atoms: A: -x,-y+2,-z.   B: x-1,y,z

Table 3. Selected bond distances (Å) and angles (˚) for the structure of $[CH_6N_3]_3[Ru_2(bipy)_2(CN)_7]\bullet 2H_2O$

Ru(1)-C(13)	1.973(2)	Ru(2)-C(26)	1.972(2)
Ru(1)-C(12)	1.983(2)	Ru(2)-C(27)	1.985(2)
Ru(1)-C(11)	1.997(2)	Ru(2)-C(25)	1.995(2)
Ru(1)-C(14)	2.0569(19)	Ru(2)-N(6)	2.063(2)
Ru(1)-N(1)	2.1173(17)	Ru(2)-N(8)	2.1170(17)
Ru(1)-N(2)	2.1186(18)	Ru(2)-N(7)	2.1194(18)

C(13)-Ru(1)-C(12)	91.43(8)	C(26)-Ru(2)-C(27)	91.42(8)
C(13)-Ru(1)-C(11)	87.61(9)	C(26)-Ru(2)-C(25)	87.66(9)
C(12)-Ru(1)-C(11)	88.31(8)	C(27)-Ru(2)-C(25)	88.52(8)
C(13)-Ru(1)-C(14)	92.82(8)	C(26)-Ru(2)-N(6)	92.81(8)
C(12)-Ru(1)-C(14)	89.07(8)	C(27)-Ru(2)-N(6)	88.93(8)
C(11)-Ru(1)-C(14)	177.36(8)	C(25)-Ru(2)-N(6)	177.42(8)
C(13)-Ru(1)-N(1)	94.72(8)	C(26)-Ru(2)-N(8)	94.80(8)
C(12)-Ru(1)-N(1)	172.02(8)	C(27)-Ru(2)-N(8)	171.97(8)
C(11)-Ru(1)-N(1)	97.01(7)	C(25)-Ru(2)-N(8)	96.79(7)
C(14)-Ru(1)-N(1)	85.56(7)	N(6)-Ru(2)-N(8)	85.70(7)
C(13)-Ru(1)-N(2)	171.86(8)	C(26)-Ru(2)-N(7)	171.89(8)
C(12)-Ru(1)-N(2)	96.69(7)	C(27)-Ru(2)-N(7)	96.67(7)
C(11)-Ru(1)-N(2)	93.24(8)	C(25)-Ru(2)-N(7)	93.07(8)
C(14)-Ru(1)-N(2)	86.71(7)	N(6)-Ru(2)-N(7)	86.83(7)
N(1)-Ru(1)-N(2)	77.14(7)	N(8)-Ru(2)-N(7)	77.09(7)

Table 4. Selected bond distances (Å) and angles (˚) for the structure of $[CH_6N_3]_2[Ru(^tBu_2bipy)(CN)_4]\cdot 2H_2O$

Ru(1)-C(4)	1.978(4)	Ru(1)-C(2)	2.051(6)
Ru(1)-C(3)	1.984(4)	Ru(1)-N(21)	2.105(3)
Ru(1)-C(1)	2.038(5)	Ru(1)-N(11)	2.109(3)

C(4)-Ru(1)-C(3)	89.90(15)	C(1)-Ru(1)-N(21)	91.76(14)
C(4)-Ru(1)-C(1)	87.85(15)	C(2)-Ru(1)-N(21)	90.65(15)
C(3)-Ru(1)-C(1)	87.60(18)	C(4)-Ru(1)-N(11)	173.61(14)
C(4)-Ru(1)-C(2)	91.1(2)	C(3)-Ru(1)-N(11)	96.44(14)
C(3)-Ru(1)-C(2)	90.10(19)	C(1)-Ru(1)-N(11)	91.60(17)
C(1)-Ru(1)-C(2)	177.49(16)	C(2)-Ru(1)-N(11)	89.7(2)
C(4)-Ru(1)-N(21)	97.51(13)	N(21)-Ru(1)-N(11)	76.13(12)
C(3)-Ru(1)-N(21)	172.53(14)		

Table 5. Crystal, data collection and refinement data for the four crystal structures.

Complex	$[Nd(H_2O)_{5.5}][Ru_2(bipy)_2(CN)_7]$• $11H_2O$	$[Pr(H_2O)_6][Ru_2(phen)_2(CN)_7]$ •$9H_2O$
Formula	$C_{27}H_{49}N_{11}NdO_{16.5}Ru_2$	$C_{31}H_{46}N_{11}O_{15}PrRu_2$
Molecular weight	1138.15	1155.84
Crystal system	Monoclinic	Monoclinic
Space group	*P*2(1)/n	*P*2(1)/n
T, K	100(2)	150(2)
a, Å	10.3228(2)	10.3796(3)
b, Å	29.6019(4)	31.0096(9)
c, Å	14.7554(2)	14.8454(5)
β,°	107.8130(10)	108.263(2)
V, $Å^3$	4292.72(12)	4537.6(2)
Z	4	4
ρ, g cm^{-3}	1.761	1.692
Crystal size, mm^3	0.2 x 0.1 x 0.1	0.07 x 0.04 x 0.04
μ, mm^{-1}	1.964	1.787
Unique data, restraints, parameters	7935, 35, 604	7996, 0, 559
Final *R*1, *wR*2[a]	0.0443, 0.1133	0.0639, 0.1779

Complex	$[CH_6N_3]_3[Ru_2(bipy)_2(CN)_7]$• $2H_2O$	$[CH_6N_3]_2[Ru(^tBu_2bipy)(CN)]$ •$2H_2O$
Formula	$C_{30}H_{38}N_{20}O_2Ru_2$	$C_{24}H_{40}N_{12}O_2Ru$
Molecular weight	912.94	629.75
Crystal system	150(2)	150(2)
Space group	Monoclinic	Monoclinic
T, K	*P*2(1)/c	*P*2(1)/c
a, Å	14.8630(10)	14.0627(4)
b, Å	11.4003(8)	17.6156(6)
c, Å	22.2687(15)	12.3573(4)
β,°	90.072(3)	101.669(2)
V, $Å^3$	3773.3(4)	2997.92(16)
Z	4	4
ρ, g cm^{-3}	1.607	1.395
Crystal size, mm^3	0.3 x 0.1 x 0.1	0.1 x 0.2 x 0.2
μ, mm^{-1}	0.859	0.566
Unique data, restraints, parameters	8744, 0, 482	8991, 15, 424
Final *R*1, *wR*2[a]	0.0274, 0.0718	0.0593, 0.1708

a The value of R1 is based on selected data with $I > 2\sigma(I)$; the value of wR2 is based on all data.

Table 6. Variations in intensities of principal peaks for mononuclear *vs*. dinuclear complex anions according to ES mass spectra, for reactions under different conditions.

m/z observed	*m/z* calcd.	Species	Relative abundance %		
			A	B	C
438	437.9	$[Ru(phen)(CN)_3K_2]^+$	20	12	50
464	463.9	$[Ru(phen)(CN)_4K_2]^+$	2	30	-
503	502.9	$[Ru(phen)(CN)_4K_3]^+$	100	100	72
902	901.8	$[Ru_2(phen)_2(CN)_7K_4]^+$	2	4	100
967	966.8	$[Ru_2(phen)_2(CN)_7K_4 + KCN]^+$	1	17	-

A: Normal conditions (pH 3, reaction time 24h)

B: Longer time (pH 3, reaction time 3 days)

C: Lower pH and longer time (pH 2, reaction time 3 days)

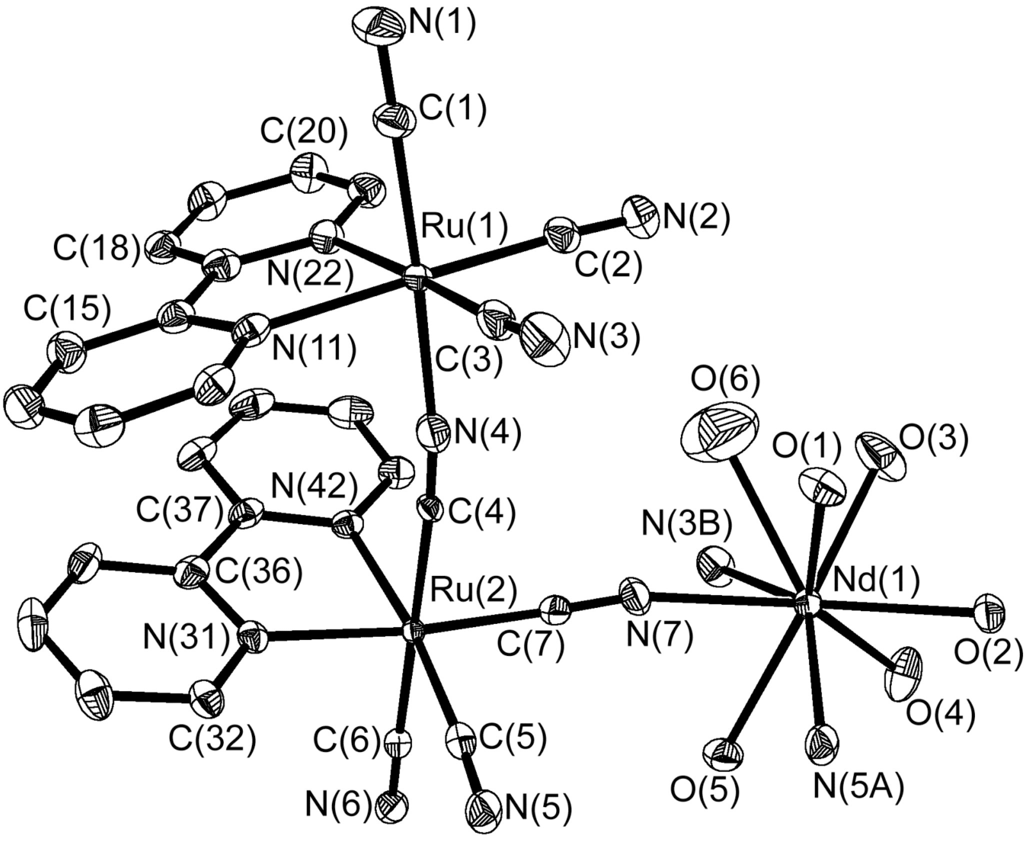
N(1)
C(1)
C(20)
Ru(1)
N(2)
C(18)
N(22)
C(2)
C(15)
N(11)
C(3)
N(3)
O(6)
N(4)
O(1)
O(3)
N(42)
C(37)
C(4)
N(3B)
C(36)
Nd(1)
Ru(2)
N(31)
C(7)
N(7)
O(2)
O(4)
C(32)
C(6)
C(5)
N(6)
N(5)
O(5)
N(5A)

Fig. 1

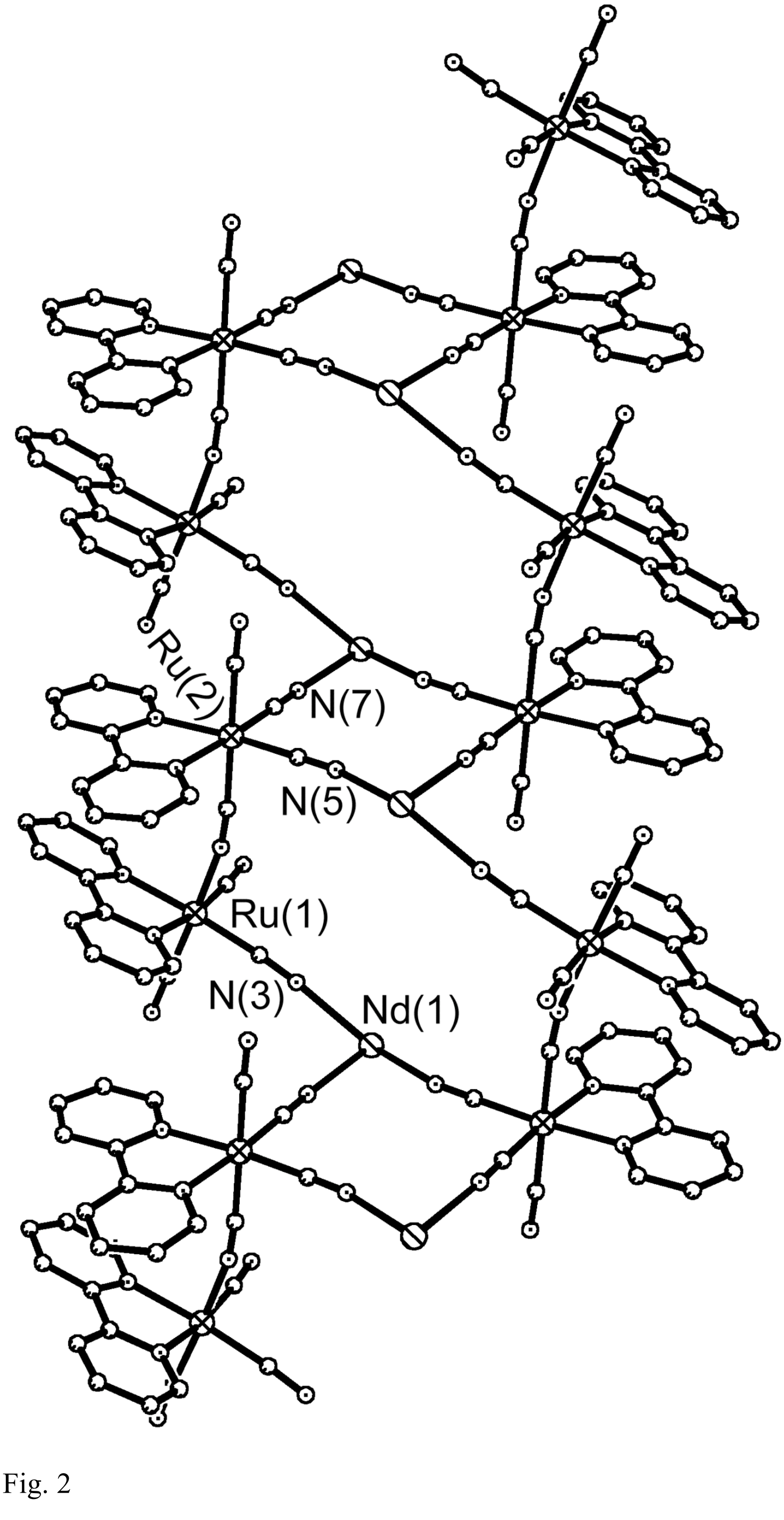

Fig. 2

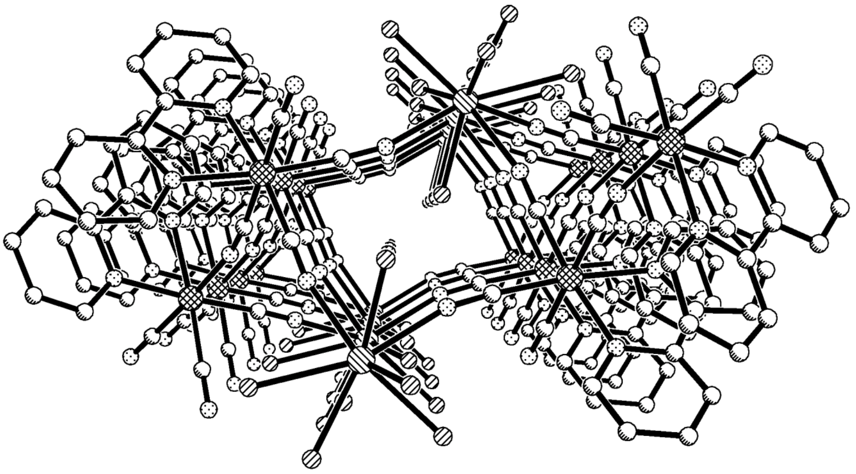

Fig. 3

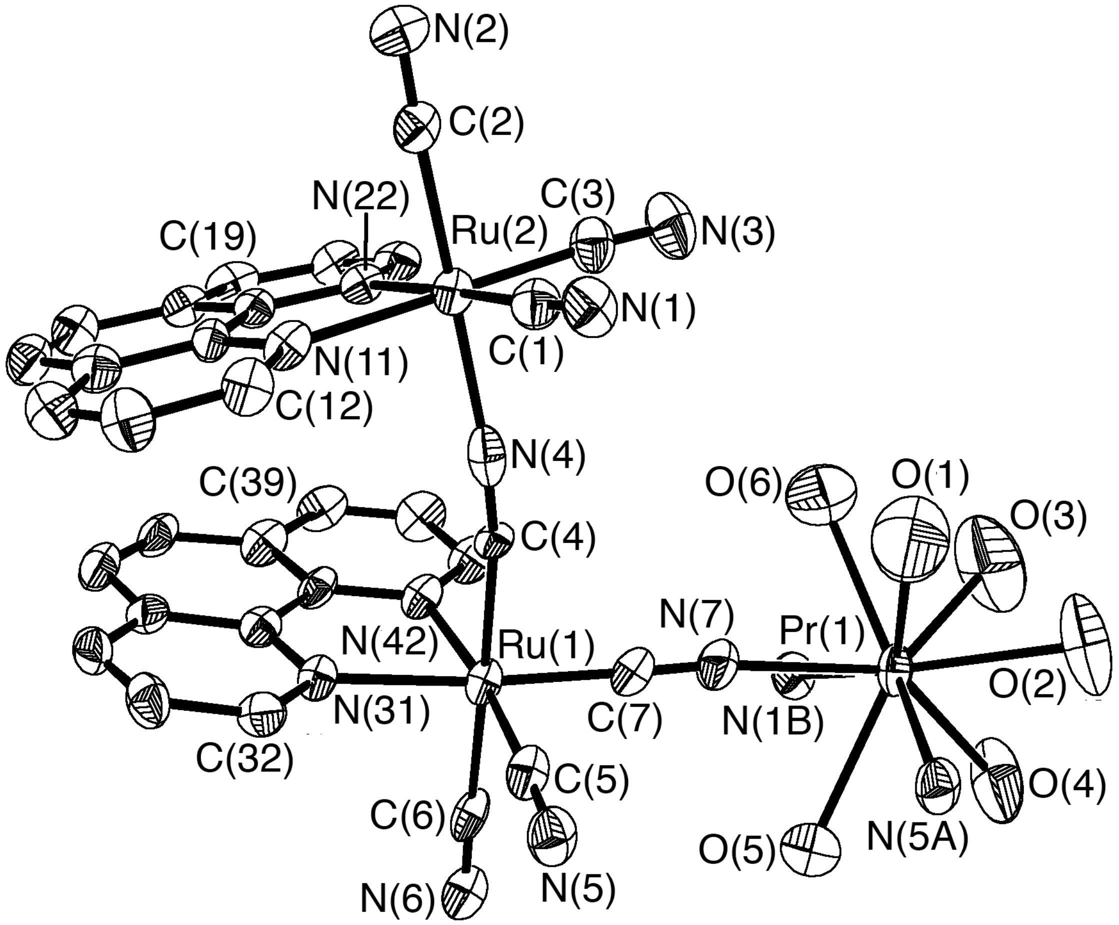
N(2)
C(2)
N(22)
C(3)
Ru(2)
N(3)
C(19)
N(1)
N(11)
C(1)
C(12)
N(4)
O(6)
O(1)
C(39)
O(3)
C(4)
N(7)
Pr(1)
N(42)
Ru(1)
O(2)
N(31)
C(7)
N(1B)
C(32)
C(5)
O(4)
C(6)
O(5)
N(5A)
N(6)
N(5)

Fig. 4

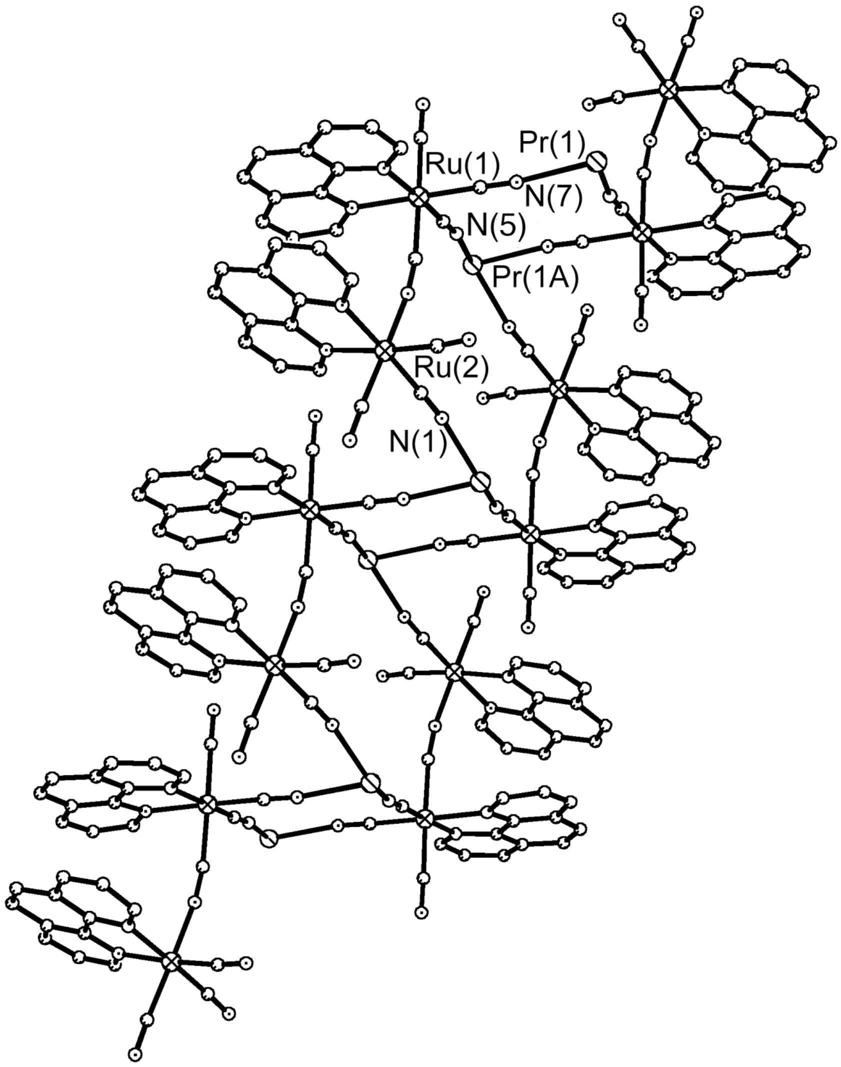

Fig. 5

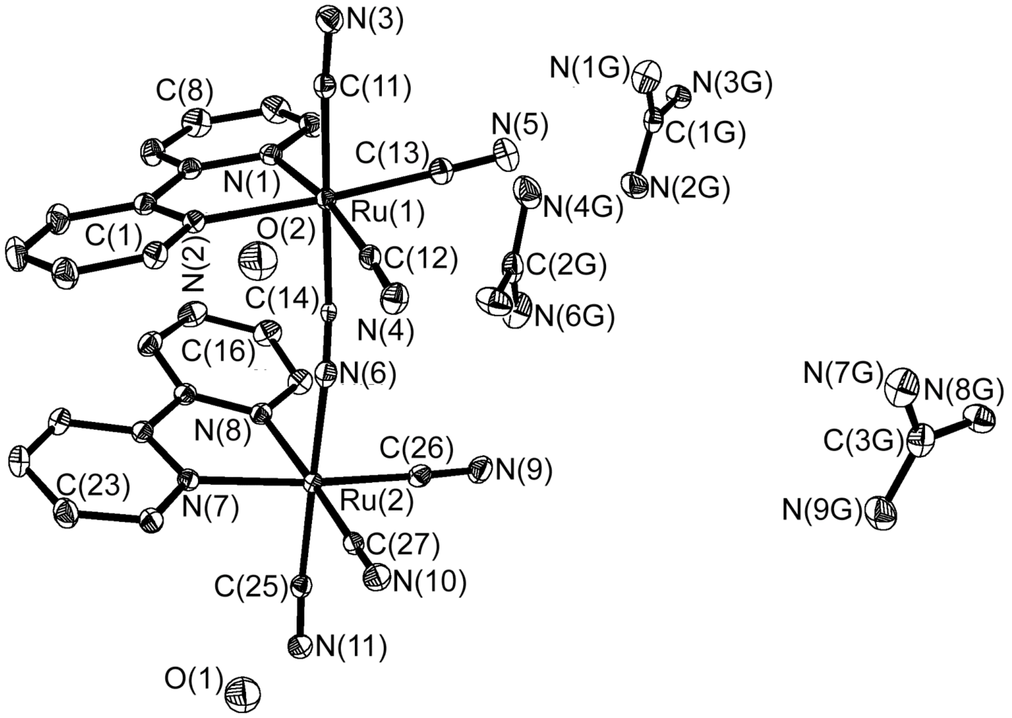
N(3)
C(11)
C(8)
N(1G)
N(3G)
C(1G)
C(13)
N(5)
N(1)
N(4G)
N(2G)
Ru(1)
C(1)
O(2)
C(12)
N(2)
C(2G)
C(14)
N(6G)
N(4)
C(16)
N(6)
N(7G)
N(8G)
N(8)
C(3G)
C(26)
N(9)
C(23)
Ru(2)
N(7)
N(9G)
C(27)
C(25)
N(10)
N(11)
O(1)

Figure 6

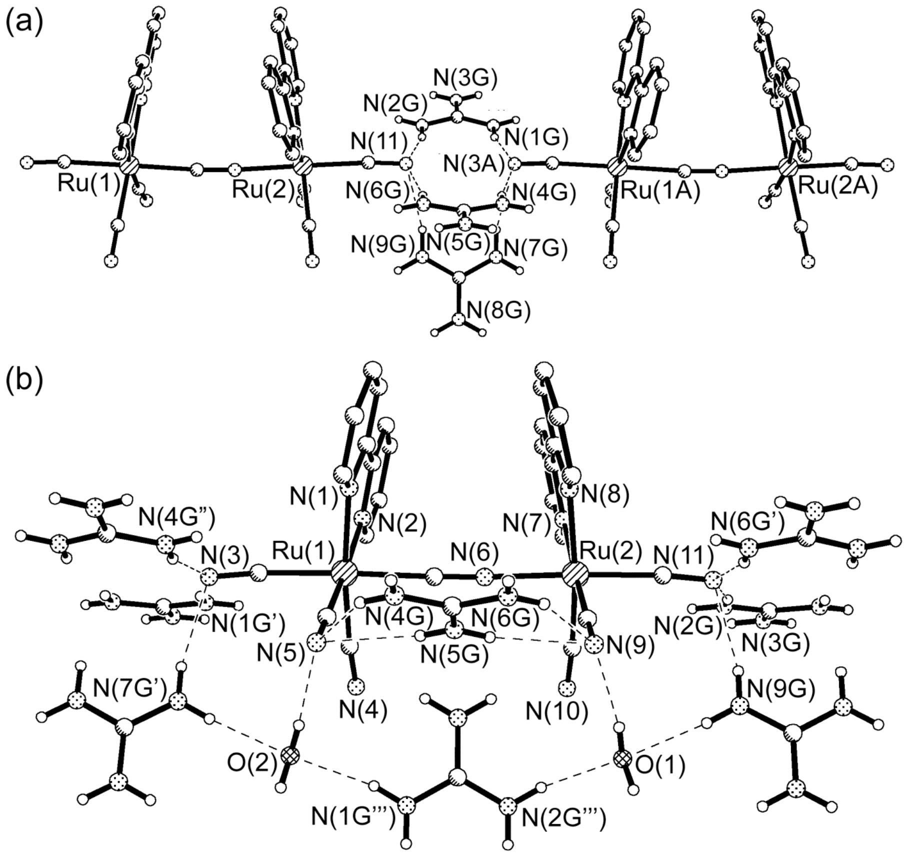
(a)
N(3G)
N(2G)
N(11)
N(1G)
N(3A)
Ru(1)
Ru(2)
N(6G)
N(4G)
Ru(1A)
Ru(2A)
N(9G)
N(5G)
N(7G)
N(8G)
(b)
N(1)
N(8)
N(2)
N(7)
N(4G")
N(6G')
N(3)
Ru(1)
N(6)
Ru(2)
N(11)
N(1G')
N(4G)
N(6G)
N(2G)
N(5)
N(5G)
N(9)
N(3G)
N(7G')
N(9G)
N(4)
N(10)
O(2)
O(1)
N(1G''')
N(2G''')

Fig. 7

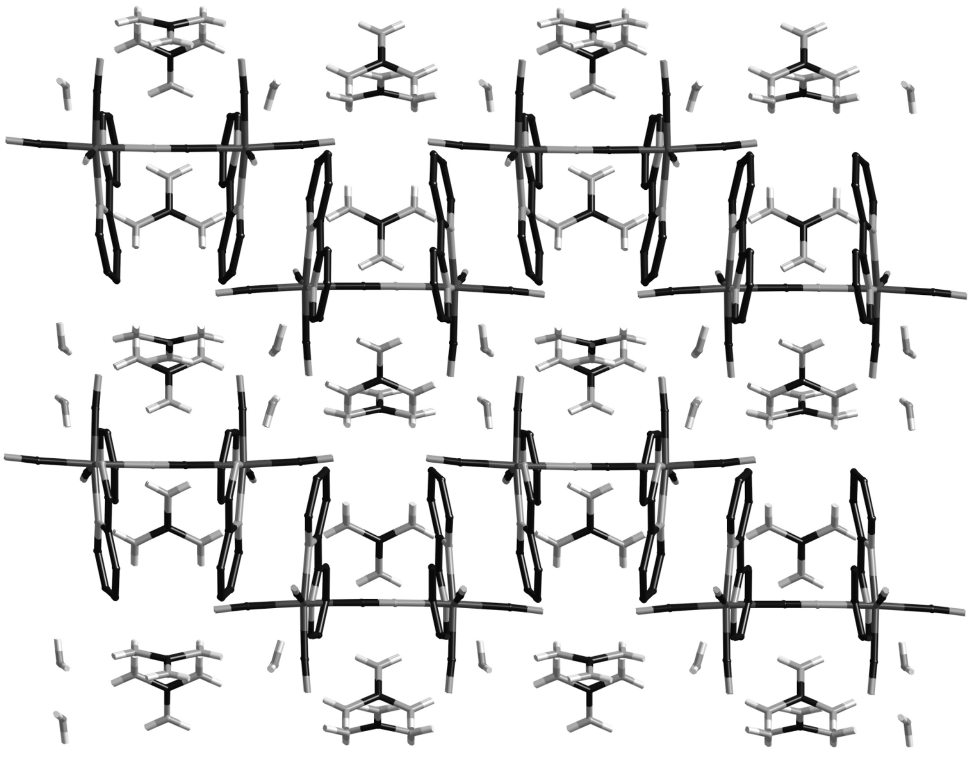

Fig. 8

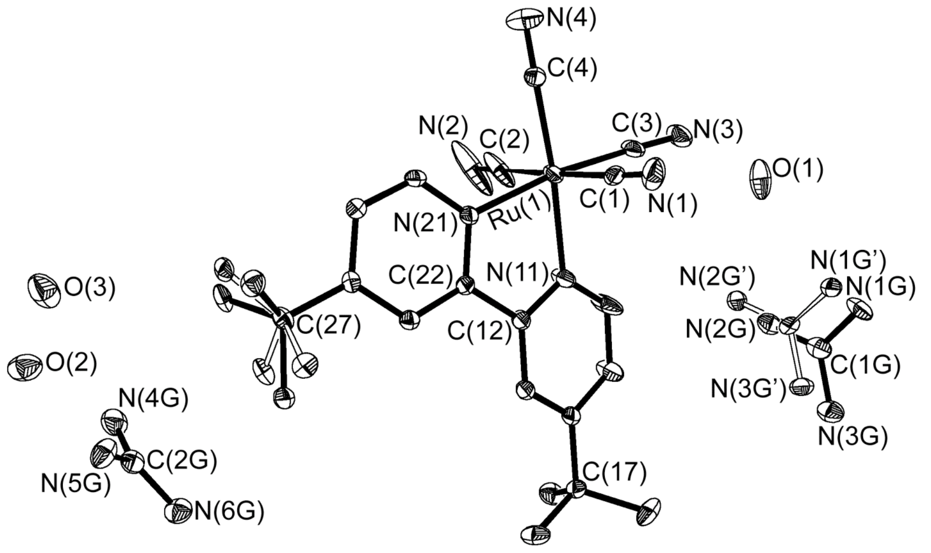
N(4)
C(4)
N(2)
C(2)
C(3)
N(3)
O(1)
Ru(1)
C(1)
N(1)
N(21)
O(3)
C(22)
N(11)
N(2G')
N(1G')
N(1G)
C(27)
C(12)
N(2G)
O(2)
C(1G)
N(3G')
N(4G)
N(3G)
C(2G)
N(5G)
C(17)
N(6G)

Fig. 9

Formation and structural chemistry of the unusual cyanide-bridged dinuclear species $[Ru_2(\mathbf{NN})_2(CN)_7]^{3-}$ (**NN** = 2,2'-bipyridine or 1,10-phenanthroline)

Sofia Derossi, Svetlana G. Baca, Thomas A. Miller, Harry Adams,
John C. Jeffery, and Michael D. Ward[a,*]

Graphical abstract for Table of Contents

During crystallisation of $[Ru(\mathbf{NN})(CN)_4]^{2-}$ (**NN** = 2,2'-bipyridine or 1,10-phenanthroline) with Lewis-acidic cations [Ln(III), guanidinium] the cyanide-bridged dimers $[Ru_2(\mathbf{NN})_2(CN)_7]^{3-}$ form, which generate one-dimensional coordination polymers with Ln(III) cations or a hydrogen-bonded network with guanidinium cations.